Vapor Phase Epitaxy, Real-time Process Monitoring by P-Polarized Reflectance Spectroscopy and Closed-loop Control of

Controlling and optimizing growth processes require improved methods of characterization and understanding of decomposition pathways and surface reaction kinetics. They also require the development of advanced nonlinear filtering and feedback control concepts. This contribution describes results on real-time optical monitoring of thin film growth processes by p-polarized reflectance (PR) using a pulsed chemical beam epitaxy (PCBE) approach, where the growth surface is sequentially exposed to organometallic precursors. Under these conditions the surface reaction kinetics can be followed by analyzing a periodically (in composition and thickness) modulated surface reaction layer (SRL). This modulation can be captured in the PR signals as a fine structure that is superimposed to the interference fringes produced by underlying growing film. The optical response is linked to the growth process via a reduced order surface kinetics (ROSK) model and integrated as a control signal in the implementation of filter and control algorithms for closed-loop controlled growth. The control concept has been applied for thickness and compositional graded multi-heterostructure $Ga_xIn_{1-x}P$ epilayers and validated by *ex situ* post-growth analysis. This results in superior tracking of composition and thickness targets under closed-loop controlled conditions when compared to films grown using predesigned source injection profiles (open-loop conditions).

1. Introduction

Real-time optical characterization of thin film inherits the challenge of relating macroscopic optical signatures to microscopic surface chemistry processes that drive the growth process, to growth/film properties, such as composition, instantaneous growth rate, or structural layer quality. The need for stringent tolerances in control of film thickness and composition is especially acute for chemical deposition methods, where organometallic precursor decomposition at the growth surface dominates the nucleation kinetics, surface atom mobility, and steady-state growth reaction kinetics. The limited knowledge about kinetics of nucleation and deposition has impeded progress in understanding and controlling thin film growth. To improve the understanding of the driving mechanisms of growth processes, nonintrusive real-time techniques have been developed. The focus has been on the monitoring of surface processes by reflection high energy electron diffraction (RHEED) (Yoshimoto *et al.* 1994), reflectance difference spectroscopy (RDS) (Aspnes *et al.* 1988), surface photo absorption (SPA) (Kobayashi and Horikoshi 1989, 1990; Kobayashi *et al.* 1991) and p-polarized reflectance spectroscopy, PRS (Dietz and Bachmann 1995, 1996; Dietz *et al.* 1997).

Presently, the only two techniques that combine the advantage of high surface sensitivity with bulk film properties characterization are (i) an integrated spectral ellipsometry (SE)/RDS spectrometer developed by Aspnes *et al.* (Aspnes 1996, Ebert *et al.* 2000) and (ii) PRS (Dietz and Bachmann 1995). Both techniques aim to integrate the optical response to surface processes with the optical response to bulk properties to monitor and control the deposition process with submonolayer resolution.

This contribution describes p-polarized reflectance spectroscopy (PRS) for closed-loop deposition control during pulsed chemical beam epitaxy (PCBE) using III–V heteroepitaxial growth as an example. The demonstrated high sensitivity of PRS towards surface reactions processes in the context of real-time monitoring of PCBE has opened new possibilities for characterization and control of thin film deposition processes. For instance, during heteroepitaxial $GaP/Ga_xIn_{1-x}P$ growth on silicon under PCBE conditions the surface is periodically exposed to metal-organic precursors, which causes a periodic alteration in composition and thickness of the surface reaction layer (SRL). The control of a growth process using the optical signature from the SRL that feeds the underlying growth requires detailed instantaneous simulation and prediction of the surface chemistry and its link to the optical properties of the outermost layer in a multilayer medium. A reduced order surface kinetics (ROSK) model has been developed that describes the growth process with a mathematically reduced number of surface reaction equations using heteroepitaxial $Ga_xIn_{1-x}P$ growth as an example. The dynamics in the molar concentrations of surface constituents evolution gives information on SRL thickness, its optical response in a four-media layer approximation, the instantaneous growth rate, and the composition of the growing film. For real-time closed-loop deposition control a virtual substrate approach has been used, an approach introduced by D. E. Aspnes for product-driven deposition control (see *III–V Epitaxy, Monitoring and Closed-Loop Feedback Control of Spectroscopic Ellipsometry of*).

2. Growth Monitoring By p-Polarized Reflection Spectroscopy

For monitoring both the bulk and surface properties during heteroepitaxial $Ga_xIn_{1-x}P$ growth on silicon, PRS together with laser light scattering (LLS) has been integrated in a PCBE system as schematically depicted in Fig. 1. During heteroepitaxial $Ga_xIn_{1-x}P$ growth on silicon PCBE conditions, the surface of the

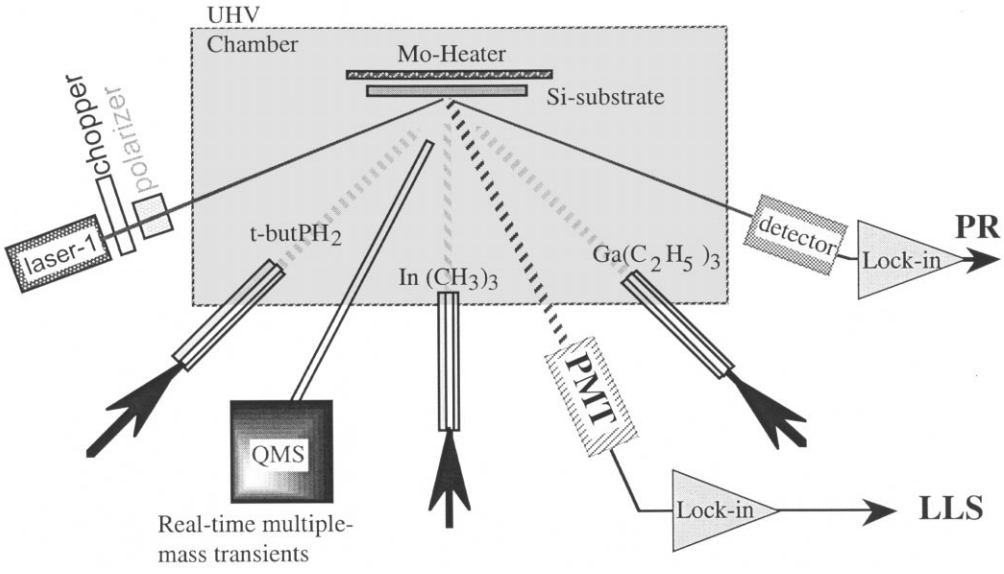

Figure 1
Schematic setup of growth monitoring by PRS, LLS, and QMS for III–V compound semiconductor growth under PCBE growth conditions.

substrate is exposed to pulsed ballistic beams of TBP ($(C_4H_9)PH_2$), TEG ($Ga(C_2H_5)_3$) and TMI ($In(CH_3)_3$) at typically 350–470 °C. The total pressure during growth in the reactor is kept in the range of 10^{-3}–10^{-4} mbar and all precursors are supplied sequentially separated by pauses. In Fig. 2 the typical evolution of the PR signals during growth of $Ga_{1-x}In_xP/GaP$ on Si(001) at 420 °C, recorded for PR70 and PR75 at $\lambda = 650\,\text{nm} \pm 5\,\text{nm}$ and at $\lambda = 632.8\,\text{nm}$ respectively, is presented. The growth process is composed of three stages:

(i) substrate and surface preconditioning;

(ii) deposition of a GaP buffer layer lattice-matched to the substrate; and

(iii) growth of a $Ga_{1-x}In_xP$ layer with a fixed composition x.

During the preconditioning period, the PR signals change in response to the temperature dependency of the dielectric function of the substrate. After initiating growth, interference fringes are observed in the temporal evolution of the PR signals as the film growth progresses. Note in Fig. 2 that both PR signals are phase shifted owing to the fact that one angle of incidence (PR75) is above—and the other (PR70) below—the pseudo-Brewster angle of the growing film material. As in the graph insets of Fig. 2, superimposed on the interference oscillations of the reflected intensity is a fine structure that is strongly correlated to the timing sequence of the precursors employed, as their effects contribute to the growth surface.

In addition, the amplitude of the fine structure undergoes at least two modulations: (i) a modulation in amplitude owing to the exposure of the growth surface to different doses and different species of precursors, and (ii) a long-period modulation of the fine structure tagged to the position on the interference fringe. The first effect contains information about surface relevant constituents related to instantaneous growth and film composition and is discussed in more detail below. The second effect can be modeled as a superficial overlayer containing the average optical properties and thickness of a surface reaction layer feeding the underlying growth process (Beeler *et al.* 1999).

The correlation of the PR fine structure with the precursor pulsing sequence is shown in Fig. 3 for various TMI:TEG flow ratios. The PR responses are taken from several different growth experiments on the increasing flank of the PR_70 interference fringe. The increase in slope with increasing TMI:TEG ratio correlates to increase in growth rate per cycle sequence, while the change in the fine structure response to the individual precursor pulse relates to the change in molar concentrations of constituents in the surface reaction layer. We observe that the PR fine structure response not only depends on the molar concentrations of constituents in the surface reaction layer but also on the optical response factors for each constituent, associated with transitions characteristic for each specific molecular fragment. As depicted in Fig. 3, the approximate same flux of TMI and TEG (TMI:TEG ratio = 1) results in different PR amplitude changes. Under steady-state growth conditions, the observed differences in amplitude height are

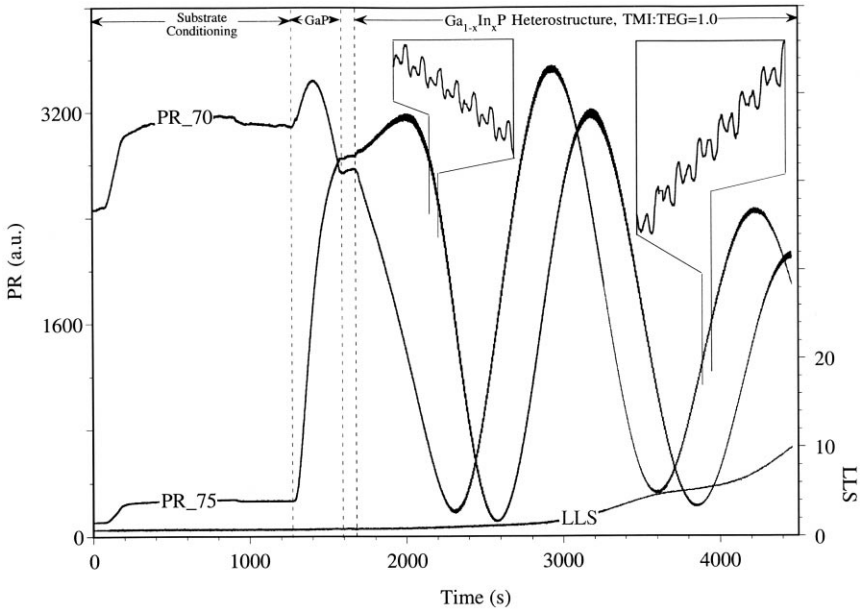

Figure 2
Heteroepitaxial $Ga_{1-x}In_xP$/GaP growth on Si(001) monitored by PR at two angles of incidence and by LLS.

correlated to concentration of surface constituents and their optical response factors as discussed in the next section. Effects related to differences in surface sites and mobility are neglected.

3. *Reduced Order Surface Kinetics (ROSK) Model For $Ga_{1-x}In_xP$ Growth*

A surface kinetics model for the ternary compound semiconductor $Ga_xIn_{1-x}P$ growth from trimethylindium (TMI), triethylgallium (TEG), and tertiarybutylphosphine TBP ($(C_4H_9)PH_2$) must describe the surface defragmentation processes of employed precursors, the chemical reactions between the precursor fragments, and the incorporation of the surface constituents in the underlying growing film. The relevant regions are depicted in Fig. 4. For growth under low-pressure CVD conditions, the precursor decomposition process can be described in first order by surface reactions and no gas phase reactions have to be considered.

The understanding and control of the kinetics of heteroepitaxy requires detailed information on the surface structure that depends on both reconstruction and the nature and distribution of defects in the epitaxial film. Several studies on the pyrolysis of TEG (Murrell *et al.* 1990), TMI and TBP (Li *et al.* 1989), on GaAs (Murrell *et al.* 1990, McCaulley and Donnelly 1991), InP (Larsen *et al.* 1987), GaP (Li *et al.* 1989, Garcia *et al.* 1991), and silicon (Lin *et al.* 1989) surfaces have been reported. However, the progress in understanding and controlling thin film growth has been very slow, because little is known about chemical reaction pathways and reaction kinetics parameters during the decomposition process of the organometallic precursors.

The reduced order surface kinetics (ROSK) model for GaP (Beeler *et al.* 1999) and $Ga_xIn_{1-x}P$ (Dietz *et al.* 1999) under PCBE growth conditions that are used embodies the simplifying assumption that many reactions which make up the TBP pyrolysis are combined into one step and the reactions which make up the TEG and the TMI decomposition are combined into two steps for each precursor. The formation of $Ga_xIn_{1-x}P$ is one final step made up from the formation of the binaries GaP and InP. The process is driven by a periodic source vapor cycle as schematically shown in Fig. 3. The resulting kinetic model representing the SRL reactions is given by the following system of ordinary differential equations:

$$\frac{\mathrm{d}}{\mathrm{d}t}n_1(t) = u_{\mathrm{TBP}} - \tilde{a}_1 n_1(t) - \tilde{a}_4 n_3(t) n_1(t) - \tilde{a}_6 n_7(t) n_1(t) \tag{1}$$

$$\frac{\mathrm{d}}{\mathrm{d}t}n_2(t) = u_{\mathrm{TEG}} - \tilde{a}_2 n_2(t) \tag{2}$$

$$\frac{\mathrm{d}}{\mathrm{d}t}n_3(t) = \tilde{a}_2 n_2(t) - \tilde{a}_3 n_3(t) - \tilde{a}_4 n_3(t) n_1(t) \tag{3}$$

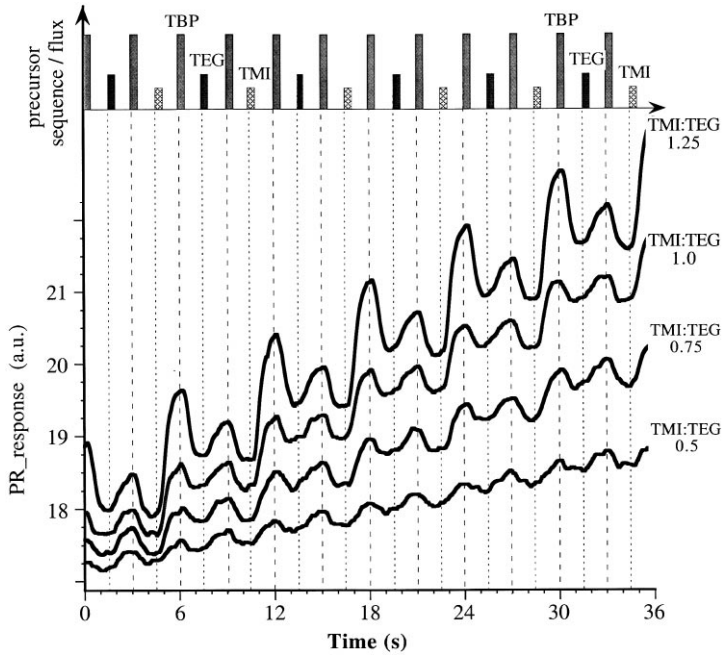

Figure 3
Schematic representation of a precursor cycle sequence used for the growth of the ternary compound semiconductor $Ga_{1-x}In_xP$ grown via the organometallic precursors TBP, TEG, and TMI.

$$\frac{d}{dt}n_5(t) = u_{TMI} - k_5 n_5(t) \tag{4}$$

$$\frac{d}{dt}n_6(t) = \tilde{a}_5 n_5(t) - \tilde{a}_6 n_6(t) - \tilde{a}_7 n_6(t) n_1(t) \tag{5}$$

with the two incorporation reactions

$$\frac{d}{dt}n_4(t) = \tilde{a}_4 n_3(t) n_1(t) \tag{6}$$

$$\frac{d}{dt}n_7(t) = \tilde{a}_7 n_6(t) n_1(t) \tag{7}$$

for GaP and InP, respectively.

The variables n_1, n_2, n_3, n_5, and n_6 represent the number of moles of the surface constituent in the SRL. The periodic supply functions expressed in terms of the molar concentration of TBP, TEG, and TMI reaching the surface are denoted by u_{TBP}, n_{TEG}, and n_{TMI}, respectively. The system of differential Eqns. (1) to (5) approximate the decomposition kinetics, taking in account desorption losses for the arriving precursors and for intermediate products. The differential Eqns. (6) and (5) contain the reaction terms for forming GaP and InP, using two generalized reaction parameters $\tilde{a}_4$ and $\tilde{a}_7$. Note that the surface structure, number of reaction sides, and inhomogeneous reactions are not explicitly addressed at this point and are integrated into the reaction parameters $\tilde{a}_4$ and $\tilde{a}_7$. At this point, the time-dependency of the reaction parameters $\tilde{a}_4$ and $\tilde{a}_7$ are neglected for simplicity. A more accurate model would have to take into account the changes in surface reconstruction and density of reaction sites during the period of exposure of the growth surface to precursors.

The solution of this coupled differential equations system, together with appropriate initial conditions, can be obtained numerically for the number of moles n_1 to n_7. From these solutions, the film and SRL thicknesses are found. The composition, x, for the compound semiconductor $Ga_{1-x}In_xP$ is expressed as the averaged ratio of molar concentration over a cycle sequence:

$$x = \frac{\int \frac{d}{dt}n_7(t)dt}{\int \left(\frac{d}{dt}n_4(t) + \frac{d}{dt}n_7(t) \right) dt} \tag{8}$$

and the instantaneous film growth rate g_{fl} is given by

$$g_{fl} = \frac{1}{A}\left[\tilde{V}_{GaP}\frac{d}{dt}n_4(t) + \tilde{V}_{InP}\frac{d}{dt}n_7(t) \right] \tag{9}$$

where $\tilde{V}_{GaP}$ and $\tilde{V}_{InP}$ are the molar volumes for GaP

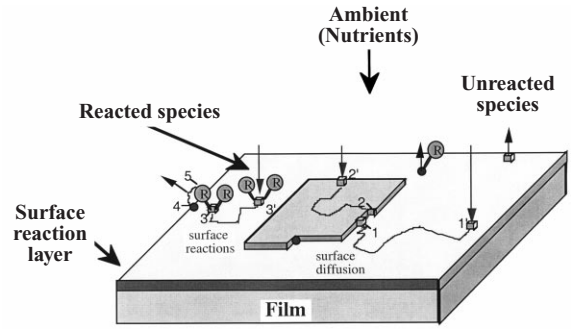

Figure 4
Relevant regions for low-pressure thin film growth utilizing metal-organic precursors: (1) the ambient; (2) the surface reaction layer, which consists of species physisorbed or chemisorbed to the surface in dynamic equilibrium with both ambient and surface and (3) the growth surface itself.

and InP, respectively. The temporal thickness evol-ution of the SRL is given by

$$d_1(t) = \frac{1}{A}\left[n_1(t)\tilde{V}_1 + n_2(t)\tilde{V}_2 + n_3(t)\tilde{V}_3 + n_5(t)\tilde{V}_5 + n_6(t)\tilde{V}_6\right] \quad (10)$$

where $\tilde{V}_i$ are the partial molar volumes of the constituents in the SRL, assumed as constants.

This surface kinetics model provides a description of how to use changes in composition and thickness of the SRL to obtain the instantaneous composition, x, and growth rate $g_{f1}(t)$ of the $Ga_xIn_{1-x}P$ film. The ROSK data can be incorporated in Fresnel's equation, which determines the reflectance amplitude, rr, of the p-polarized light, using the four-layer media composed of ambient/SRL/film/substrate combined with a virtual substrate approach as described in the following section on control methodology.

4. *Control Methodology For Thin Film Growth*

To use the real time optical observations and apply a feedback control methodology for controlling $Ga_{1-x}In_xP$ film growth, we consider a four-layer medium composed of ambient/surface-reaction layer/film/substrate as described previously (Dietz *et al.* 1999). For the case of multi-layer media of films we adapted a virtual substrate method (Aspnes 1995, 1996), where the reflectance amplitude r of the p-polarized light is given by

$$r = \frac{r_{01} - \hat{r}e^{-2i\Phi_1}}{1 + r_{01}\hat{r}e^{-2i\Phi_1}} \quad \text{with} \quad \hat{r} = \frac{r_{12} - r_k e^{-2i\Phi_2}}{1 + r_{12}r_k e^{-2i\Phi_2}} \quad (11)$$

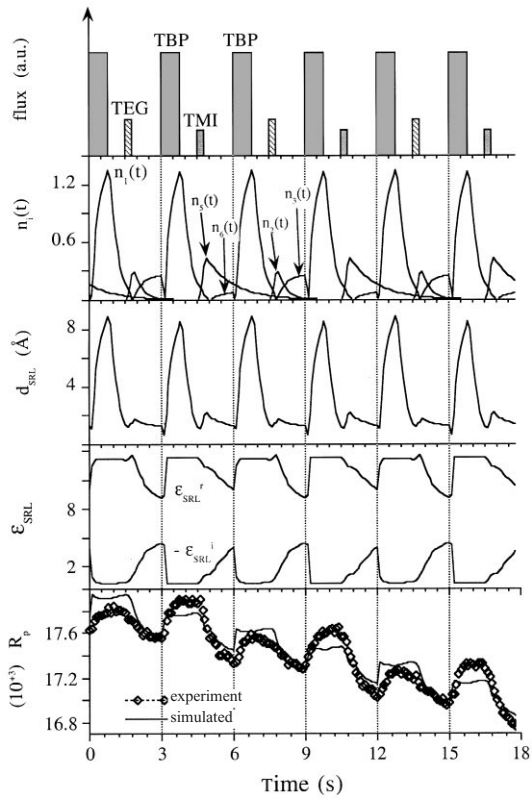

Figure 5
Simulation of surface reaction kinetics and PR response during heteroepitaxial $Ga_{1-x}In_xP$ growth on silicon under pulsed organometallic precursors exposure of TBP, TEG, and TMI. The simulated PR response is compared with experimental results obtained at $\varphi = 75.1°$, $\lambda = 632.8$ nm.

The virtual reflection index r_k is updated at the end of each cycle by

$$r_k = \frac{r_{k,k-1} - r_{k-1}e^{-2i\Phi_2}}{1 + r_{k,k-1}r_{k-1}e^{-2i\Phi_2}} \quad \text{with} \quad r_k = A_k e^{-i\theta_k} \quad (12)$$

where θ_k defines the phase factor. Based on the phase factor θ_2 the thickness d_2 of the grown layer is estimated by

$$d_2 = \frac{\lambda}{4\pi\sqrt{\varepsilon_2 - \varepsilon_0 \sin^2\phi_0}}(\theta_{\text{end}} - \theta_{\text{begin}}) \quad (13)$$

where the θ_{end}, θ_{begin} is the phase factor at the end and beginning of the layer. Similarly the growth gr_k per each cycle k is given by

$$gr_k = \frac{\lambda}{4\pi\sqrt{\varepsilon_2 - \varepsilon_0 \sin^2\phi_0}}(\theta_k - \theta_{k-1}) \quad (14)$$

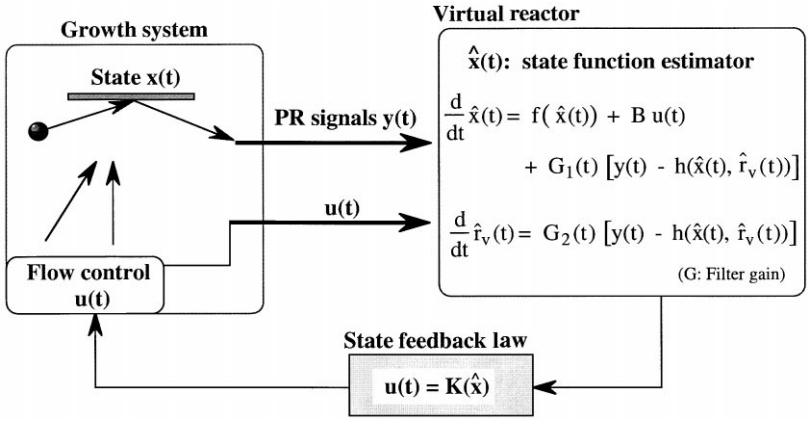

Figure 6
Control of heteroepitaxial $Ga_{1-x}In_xP$ growth: the control design consists of three elements: ROSKM described by f; filter gains $G_i(t)$ based on nonlinear-filtering techniques; and feedback law **K** based on dynamical programming.

The thickness of the specific compound is estimated by Eqn. (13) and the growth ratio of GaP and InP for each cycle determined by Eqn. (14) provides a composition estimate. A nonlinear filtering algorithm (Ito and Xiong 2000) is used for estimating the state consisting of the virtual reflection index $r_k = e^{x_1+ix_2}$, the film dielectric constant $\varepsilon = x_3 + ix_4$, and growth per cycle x_5 in real time, as schematically outlined in Fig. 6.

Let y_k denote the PR signal at the end of the kth cycle. Then the filtering problem is to estimate the signal process x^k defined by

$$\begin{pmatrix} x_1^k \\ x_2^k \\ x_3^k \\ x_4^k \\ x_5^k \end{pmatrix} = \begin{pmatrix} f_1(x^k) \\ f_2(x^k) \\ x_3^{k-1} \\ x_4^{k-1} \\ x_5^{k-1} \end{pmatrix} + \omega_k \tag{15}$$

based on the observation process $y^k = h(x^k) + v_k$.

We assume that the reflectance coefficient $|r_{k,k-1}|$ is sufficiently small at the point of evaluation, thus we can approximate Eqn. (12) and used $r_k = r_{k-1}e^{-2i\Phi_2}$ for updating the virtual index r_k. If we let f_{r_k} be the growth ratio of GaP or InP to each nominal flow rate, then the functions f_1, f_2, and h are defined by

$$f_1 + if_2 = x_1 + ix_2 + 2i\phi_2, \quad h = \frac{r_{02} + r_v}{1 + r_{02}r_v} \tag{16}$$

where $d_2 = f_{r_k}x_5$. We assume that noise processes w_k, v_k are independent (identically distributed) Gaussian random variables. The growth of GaP and InP is determined in terms of n_{GaP} and n_{InP}, which are given by

$$\frac{dn_{GaP}}{dt} = k_4 n_P n_{Ga}, \quad \frac{dn_{InP}}{dt} = k_5 n_P n_{In} \tag{17}$$

where n_P, n_{Ga}, and n_{In} denote the concentration of surface active phosphorous, gallium, and indium, respectively. We consider the model for the concentration change of active gallium in the SRL by

$$n_{Ga} = u_{TEG}S_{GaP} - n_{GaP} \tag{18}$$

where S_{GaP} is a predetermined constant. Integrating the first equation in (17), we obtain

$$n_{GaP}(t_{k+1}) = e^{-C}(n_{GaP}(t_k) - S_{GaP}u_{TEG}) + S_{GaP}u_{TEG} \tag{19}$$

where t_k is the starting time of the kth cycle and $C = k_4\int_k^{k+1} n_P(t)dt$. The rate constant k_4 varies and we estimate it in real time. We use our filtering algorithm

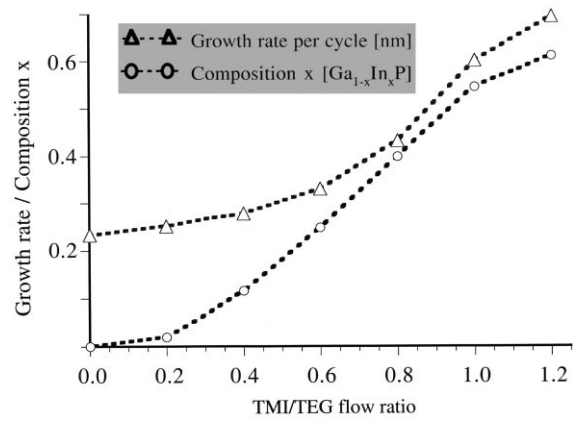

Figure 7
Composition x and growth rate of $Ga_{1-x}In_xP$ as a function of the TEG:TMI flow ratio.

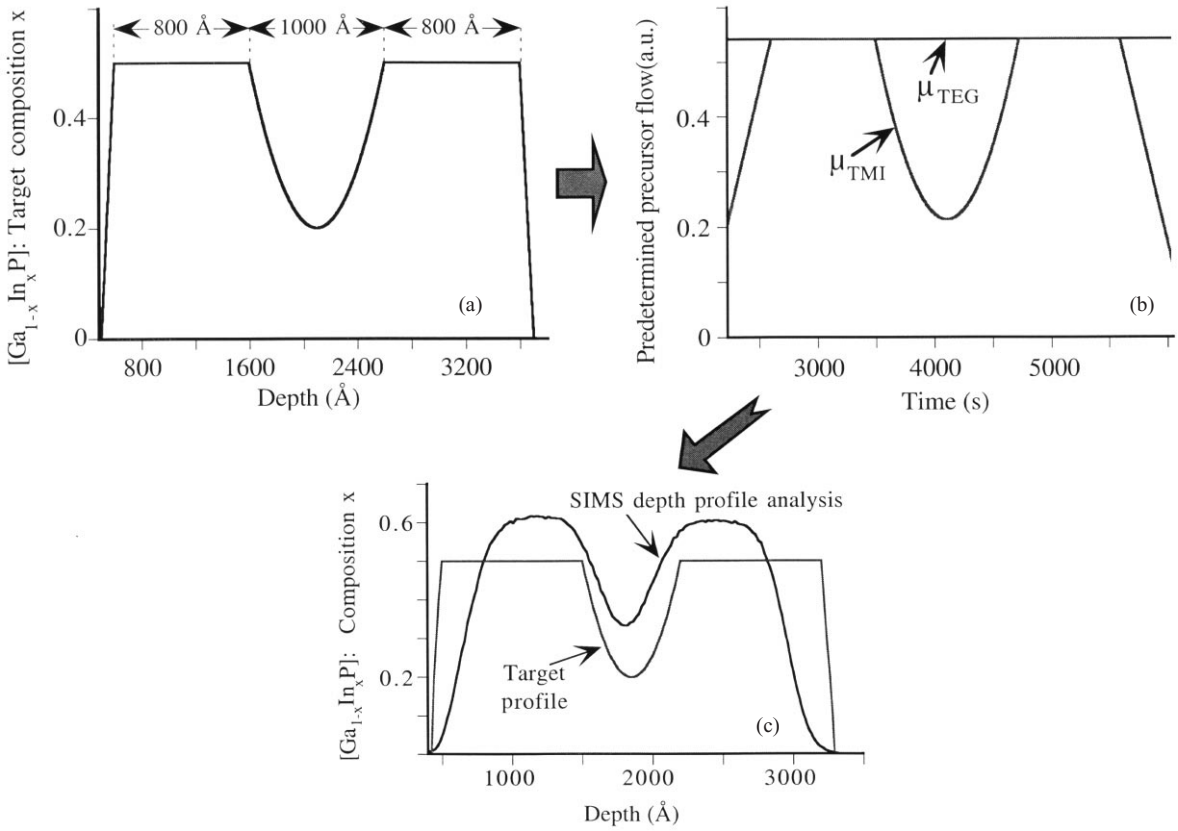

Figure 8
Open-loop control sequence (a) target profile; (b) predetermined precursor flux ratio, using competition and growth rate relation shown in Fig. 7; (c) comparison of targeted parabolic $Ga_{1-x}In_xP$ growth profile with *ex situ* SIMS depth profile analysis.

to estimate the concentration n_k of n_{GaP} and the accumulated rate constant C_k for the kth GaP cycle based on

$$\begin{pmatrix} n_k \\ C_k \end{pmatrix} = \begin{pmatrix} n_{k-1} + C_{k-1}(u_{TEG} - n_{k-1}) \\ C_{k-1} \end{pmatrix} \tag{20}$$

with measurement $gr_k = V_{GaP}nk + \tilde{v}_j$. Here gr_k is the growth rate of kth GaP cycle, determined by Eqn. (14). The growth of the InP is modeled analogously. We determine the input flow rates u^k_{TEG} and u^k_{TMI} by performing

$$\begin{aligned} &\min_{u^k_{TEG}} \left| (1+z_k)n^+_{GaP} - gr_d \right|^2 + \beta \left| u^k_{TEG} - u^{k-1}_{TEG} \right|^2, \\ &\min_{u^k_{TMI}} \left| \frac{n^+_{InP}}{n^+_{GaP}} - \frac{z_k}{1-z_k} \right|^2 + \beta \left| u^k_{TMI} - u^{k-1}_{TMI} \right|^2 \end{aligned} \tag{21}$$

subject to

$$\begin{aligned} n^+_{GaP} &= e^{-C^k_{TEG}}(n^c_{GaP} - S_{GaP}u^k_{TEG}) + S_{GaP}u^k_{TEG}, \\ n^+_{InP} &= e^{-C^k_{TMI}}(n^c_{InP} - S_{InP}u^k_{TMI}) + S_{InP}u^k_{TMI} \end{aligned} \tag{22}$$

respectively. C^k_{TEG} and C^k_{TMI} are the current estimates of C for the GaP and InP cycles respectively, and z_k is the desired composition at the k cycle. That is, we control the growth rate by u_{TEG} and then the composition by u_{TMI} for each cycle.

5. *Controlled Growth of $Ga_{1-x}In_xP$ Heterostructures*

From a series of experiments the correlation of composition and growth rate dependency as a function of flow-ratio are established. For this, epilayers with thick constant composition x in $Ga_{1-x}In_xP$ were grown and analyzed by x-ray diffraction (XRD) to obtain the compositional relationship with the established flow-ratio TMI:TEG. The growth rates were calculated from the interference fringes obtained in the PR signals. Figure 7 depicts the results of these *ex situ*

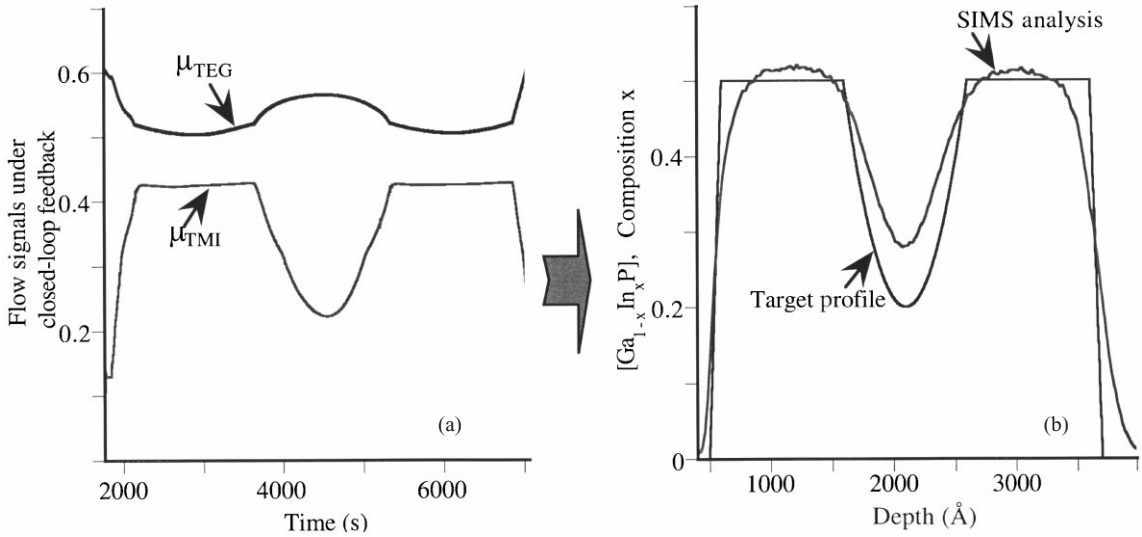

Figure 9
Closed-loop control using the same target profile as shown in Fig. 8(a). (a) Adjustment of precursor flux during closed-loop control to achieve composition and thickness target. (b) *Ex situ* SIMS depth profile analysis for a parabolic graded $Ga_{1-x}In_xP$ hetrostructure grown under closed-loop control.

analyses, clearly indicating the nonlinear correlation between growth rate and composition as a function of an established flow ratio TMI:TEG. The established correlation between growth rate and composition x with the TMI:TEG flow ratio was next used to estimate the growth parameter for compositionally graded heterostructures under open-loop control conditions. The correlation was also used as initial data base for closed-loop control.

For the growth of a parabolic $Ga_{1-x}In_xP$ heterostructure under open-loop control, a predetermined time-dependent flow profile was employed in which the flow of TEG is kept constant and the flow of TMI is varied to match desired composition and thickness. The target profile is shown in Fig. 8(a) together with the calculated time-dependent precursor flux profile for TEG and TMI in Fig. 8(b). The grown parabolic $Ga_{1-x}In_xP$ heterostructure was analyzed by secondary mass ion spectroscopy (SIMS), the depth profile of which is shown in Fig. 8(c). The instrumental broadening of approximately 50 Å and a depth integration of typically 40 Å to 50 Å leads to two errors in the SIMS analysis: (i) a compositional smear-out of profiles over 100 Å to 150 Å and (ii) the compositional dependency of the sputtering rate, which leads to an accumulative error in the depth estimate. For SIMS depth profiling using a primary Cs^+-ion beam and detecting the In^+-Cs and $^{71}Ga^{2+}$-Cs-ion intensities, the sputtering rate varies from 2.46 Å s^{-1} to 4.23 Å s^{-1} with strong compositional dependency. The error accumulation in the thickness calculation is estimated to be 10% of the film thickness, while the error in the compositional estimate is about 10% and remains independent of layer thickness, which leads to large thickness uncertainties with increasing layer thickness. The instrumental broadening factor and the given integration time leads to an error in composition, estimated to be about 10%. Even if we take these error estimates into account, the open-loop control algorithm results depicted in Fig. 8 clearly indicate a much larger discrepancy between the target profile and measured profile.

The closed-loop control algorithm uses the open-loop control parameter as initial values. However, the precursor flux values are updated in real-time integrating the real-time estimate of the optical PR-signals as described in Sect. 2. The real-time updated closed-loop control flow profile is shown in Fig. 9(a). During closed-loop control, variation of the flow of TMI is employed to control composition x while variation in the flow of TEG is used to control the growth rate. A SIMS depth profile analysis for the $Ga_{1-x}In_xP$ heterostructure so grown is shown in Fig. 9(b). The deviations from the target values are 5% in composition and about 8% in thickness. These observed deviations from the target profile lay well within the estimated error range of the SIMS profile analysis and clearly demonstrate superior tracking ability under closed-loop control, particularly in maintaining a constant composition before and after the parabolic heterostructure. For more accurate error analysis in achievable thickness and compositional control tolerances, more precise *ex situ* analysis techniques—presently not available—are needed.

6. Summary

We have described thin film growth monitoring p-polarized reflectance and demonstrated its effectiveness in compositional and thickness controlled growth of $Ga_xIn_{1-x}P$ heterostructures on silicon. A reduced-order surface kinetics model has been established to link the optical sensor to nonlinear filtering algorithm that estimates the optimal flow rates of the source vapors to achieve the desired composition and growth per cycle in real time. Parabolically graded $Ga_{1-x}In_xP$ heterostructure wells grown under open-loop and closed-loop conditions demonstrated that the on-line estimate of growth rate and composition provided by the PR probe adjusts to the nonlinearity in growth kinetics present in our system and provides better tracking to the desired profile.

Acknowledgment

Research described in this paper was supported by the DOD-MURI Grant AFOSR-F49620-95-1-0447.

Bibliography

Aspnes D E 1995 Optical approaches to the determination of composition of semiconductor alloys during epitaxy. IEEE. *J. Select. Top. Quantum Electron.* **1**, 1054–63

Aspnes D E 1996 Optical approaches to determine near-surface compositions during epitaxy. *J. Vac. Sci. Technol. A* **14**, 960–6

Aspnes D E, Harbison J P, Studna A A, Florez L T 1988 Reflectance-difference spectroscopy system for real-time measurement of crystal growth. *Appl. Phys. Lett.* **52** (12), 957–9

Beeler S, Tran H T, Dietz N 1999 Representation of GaP formation by a reduced order model using P-polarized reflectance measurements. *J. Appl. Phys.* **86**(1), 674–82

Dietz N, Bachmann K J 1995 Real-time monitoring of epitaxial processes by parallel-polarized reflectance spectroscopy. *MRS Bull.* **20**, 49–55

Dietz N, Bachmann K J 1996 p-polarized reflectance spectroscopy: a highly sensitive real-time monitoring technique to study surface kinetics under steady state epitaxial deposition conditions. *Vacuum* **47**, 133–40

Dietz N, Sukidi N, Harris C, Bachmann K J 1997 Real-time monitoring of surface processes by P-Polarized reflectance. *J. Vac. Sci. Technol. A* **15**, 807–15

Dietz N, Woods V, Ito K, Lauko I 1999 Real-time optical control of $Ga_{1-x}In_xP$ film growth by P-Polarized reflectance. *J.Vac. Sci. Technol. A* **17** (4), 1300–6

Ebert M, Bell K A, Yoo S D, Flock K, Aspnes D E 2000 In-situ monitoring of MOVPE growth by combined spectroscopic ellipsometry and reflectance difference spectroscopy. *Thin Solid Films*, in press

Garcia J C, Maurel P, Bove P, Hirtz J P 1991 Kinetic study of metalorganic molecular beam epitaxty of GaP, InP, and GaInP. *J. Appl. Phys.* **69** (5), 3297–302

Ito K, Xiong K 2000 New Gaussian filter for nonlinear filtering problems. *IEEE Trans. Automatic Control*, in press

Kobayashi N, Horikoshi Y 1989 Optical investigation on the growth process of GaAs during migration-enhanced epitaxy. *Jpn. J. Appl. Phys.* **28** (11), L1880–2

Kobayashi N, Horikoshi Y 1990 Spectral dependence of optical reflection during flow-rate modulation epitaxy of gallium arsenide by the surface photo-absorption method. *Jpn. J. Appl. Phys.* **29**, L702–L705

Kobayashi N, Makimoto T, Yamauchi Y, Horikoshi Y 1991 In-situ monitoring of gallium arsenide growth process in MOVPE by surface photo-absorption method. *J. Cryst. Growth* **107** (1–4), 62–7

Larsen C A, Buchan N I, Stringfellow G B 1987 Mass spectroscopic studies of phosphine pyrolysis and OMVPE growth of InP. *J. Cryst. Growth.* **85**, 148–53

Li S H, Buchan N I, Larsen C A, Stringfellow G B 1998 OMVPE growth mechanism for GaP using tertiarybutylphosphine and trimethylgallium. *J. Cryst. Growth* **96**, 906–14

Li S H, Larsen C A, Buchan N I, Stringfellow G B 1989 Pyrolysis of tertiarybutylphosphine. *J. Electron. Mater.* **18**, 457–64

Lin R, Gow T R, Backman A L, Cadwell L A, Lee F, Masel R I 1989 The decomposition of triethylgallium on Si(100). *J. Vac. Sci. Technol. B* **7** (4), 725–8

McCaulley R J S J A, Donnelly V M 1991 Kinetics of thermal decomposition of triethylgallium, trimethylgallium, and trimethylindium adsorbed on GaAs(100). *J. Vac. Sci. Technol. A* **9** (6), 2872–86

Murrell A J, Wee A T S, Fairbrother D H, Singh N K, Foord J S, Davies G J, Andrews D A 1990 Surface studies of the thermal decomposition of triethylgallium on GaAs (100). *J. Cryst. Growth* **105**, 199–202

Yoshimoto M, Hashimoto T, Vaccaro P, Matsunami H 1994 In-situ RHEED observation on surface reactions in laser-triggered chemical beam epitaxy of GaP. *Appl. Surf. Sci.* **79**, 227–31

H. T. Banks, N. Dietz, and K. Ito

Copyright © 2001 Elsevier Science Ltd.
All rights reserved. No part of this publication may be reproduced, stored in any retrieval system or transmitted in any form or by any means: electronic, electrostatic, magnetic tape, mechanical, photocopying, recording or otherwise, without permission in writing from the publishers.

Encyclopedia of Materials: Science and Technology
ISBN: 0-08-0431526
pp. 9488–9497